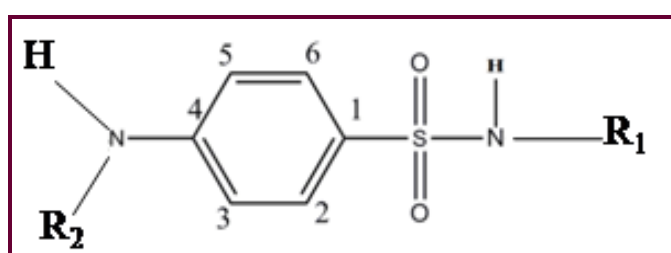


As mentioned in first chapter, to elucidate the effect of varied substituents on parent molecule (sulfonamide), to investigate the role of metal ('Ag') on different 'sulfa' derivatives and to study the polymorphs of sulfonamide– to understand the role of solvent molecule on the 'host'- author has worked out the three dimensional structure of few significant 'sulfa' compounds- three Ag complexes of sulfonamide derivatives, two polymorphs of Sulfamonomethoxine and polymorphs of Phthalylsulfacetamide and Sulfapyridine by X-ray diffraction technique. FT-IR and NMR spectra of three silver complexes are recorded. Along with these, thermogravimetric analysis and electric conductivity are measured. Quantum chemical computation using B3LYP method with different basis set is used to predict the optimized geometry and to compare with those of X-ray data for all the molecules. The contribution of intermolecular interactions towards the molecular stability has looked through Hirshfeld surface analysis for each molecule. The lattice energies associated with intermolecular interactions with two polymorphs of SMM and PHSCA are calculated by PIXEL. To correlate the structure-function relationship the silver complexes are tested for their antimicrobial activity and polymorphs are subjected to molecular docking.

The various sulfonamide derivatives with different substituents at R_1 and R_2 of the parent sulfonamide molecule (**Figure 10.1**) can be broadly categorized into the following two categories. Category –I includes the silver complexes of sulfonamide derivatives and polymorphs of sulfonamide are covered in category-II. **Figure 10.2** illustrates the different substituents for all the molecules picked up for present study.



Where R_1 and R_2 are = Functional group

Figure 10.1 Chemical structure of Sulfonamide

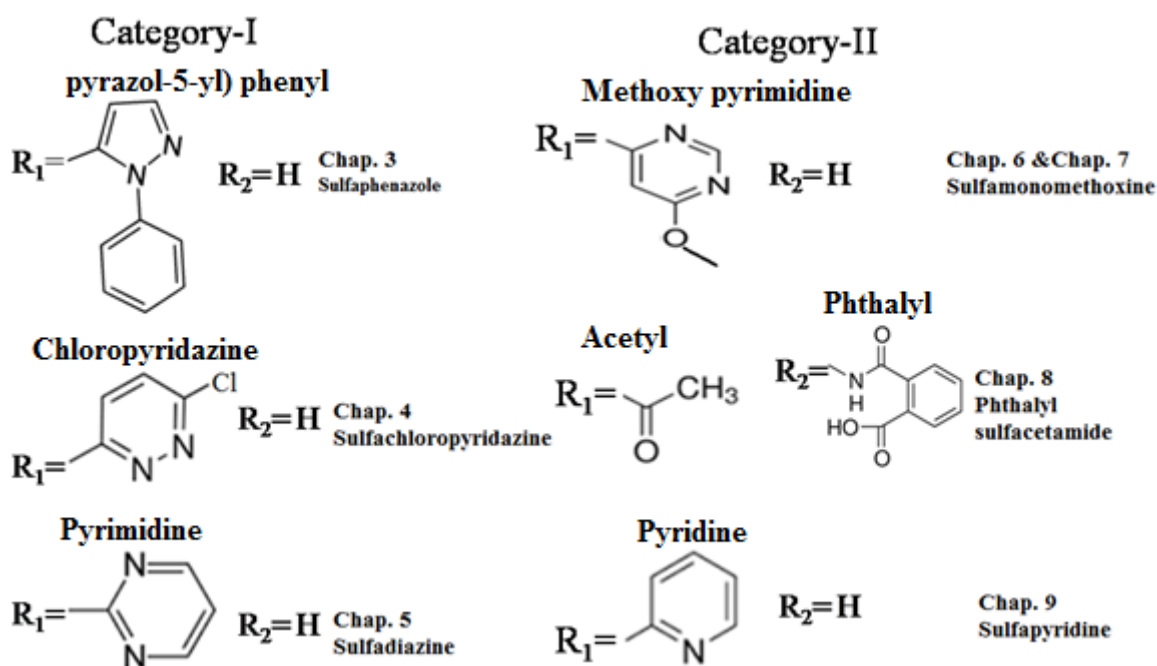


Figure 10.2 Different substituent at R_1 and R_2 for the all the molecules picked up for present study

A Precise comparison of few general features among the three ‘Ag’ complexes with different ligands have been carried out and presented in tabular form.

A. Comparison of data obtained by X-ray diffraction and by theoretical calculation for silver complexes

Comparative studies for molecular geometry and molecular conformation have been reported here. The comparative analysis of some general features like, crystal system, space group, R index, HOMO-LUMO energy, and dipole moment are tabulated in **Table 10.1**. **Table 10.2** is the comparative list for coordination geometry around silver atom. **Table 10.3(a)** and **Table 10.3(b)** present comparative list of significant bond lengths and bond angles of the silver complexes of different sulfonamide derivatives which are reported in present study. **Table 10.3(c)** summarizes comparative list of few significant torsional angles by X-ray data and by theoretical calculations at B3LYP/ LAV2p** level of theory.

Table 10.1 Comparison of few general features

Parameter	Chap.3	Chap.4	Chap.5
	AgSPZ	AgSCP	AgSDZ
Crystal system	Monoclinic	Monoclinic	Monoclinic
Space group	C2/c	P2 ₁ /c	P2 ₁ /c
R [$F^2 > 2\sigma(F^2)$]	0.0263	0.033	0.047
Goodness of fit (S)	1.08	1.03	1.36
Density (Mgm ⁻³)	1.808	1.681	1.760
HOMO energy (eV)	-5.7342	-5.6103	-5.2234
LUMO energy	-2.5162	-1.7179	-1.5187
Dipole moment (debye)	8.2808	9.6078	6.3976

Table 10.2 Coordination geometry around Ag for different silver complexes

	Ag-N (Å)	Ag-Ag (Å)	X-Ag-Y (°)
Chap. 3 AgSPZ	2.238(4)-2.362(4)		107.20(6) -133.27(6)
Chap. 4 AgSCP	2.205(2)-2.399(3)	2.8936(4)	75.3(6) – 149.2(9)
Chap. 5 AgSDZ	2.240(4)-2.617(4)	2.8892(4)	72.8(9) -175.5(9)
Ref. [192]	Ag1-N 2.229(6)-2.402(7)	3.0263(9)	75.56(7)-142.47(19)
	Ag2-N 2.211(6)-2.634(7)	3.0263(9)	59.95(18)-147.04(18)
Ref. [201]	2.195(2)-2.469(3)	2.7730(4)	78.80(5)-154.78(8)

Table 10.3(a) Significant bond lengths (Å) in the silver complexes

Bond length	Chap.3		Chap.4		Chap.5	
	X-ray	B3LYP	X-ray	B3LYP	X-ray	B3LYP
S1—O1	1.453(2)	1.607	1.437(2)	1.556	1.445(3)	1.547
S1—O2	1.458(2)	1.562	1.455(3)	1.573	1.462(3)	1.581
S1—N1	1.573(2)	1.737	1.605(2)	1.728	1.605(3)	1.743
S1—C1	1.762(2)	1.853	1.756(3)	1.844	1.769(4)	1.841
N1—C7	1.386(2)	1.391	1.373(3)	1.368	1.369(5)	1.36

Table 10.3(b) Significant bond angles (°) in the silver complexes

	Chap. 3		Chap. 4		Chap. 5	
	X-ray	B3LYP	X-ray	B3LYP	X-ray	B3LYP
O1—S1—O2	115.8(2)	114.7	115.8(4)	117.6	114.8(2)	117.7
O1—S1—N1	106.4(4)	101.1	114.3(3)	115.9	114.6(2)	115.27
O1—S1—C1	106.3(2)	106.6	107.5(3)	106.8	108.6(2)	108.9
O2—S1—N1	112.2(2)	115.9	104.7(2)	100.4	103.6(2)	99.05
O2—S1—C1	105.1(2)	109.3	108.5(2)	108.9	105.6(2)	105.38
N1—S1—C1	110.9(2)	108.6	105.4(2)	106.7	109.0(2)	109.78

Table 10.3(c) Significant torsional angles ($^{\circ}$) in the silver complexes

	Chap.3		Chap.4		Chap.5	
	X-ray	B3LYP	X-ray	B3LYP	X-ray	B3LYP
O2—S1—N1—C7	-173.8(2)	-155.2	-61.5(2)	-48.27	68.4(4)	71.07
C1—S1—N1—C7	71.15(2)	92.8	56.3(2)	70.5	-53.5(4)	-52.32
N1—S1—C1—C6	-120.3(2)	-163.6	50.4 (3)	33.7	71.9(4)	85.18

- ❖ All the three silver complexes crystallize in monoclinic system.
- ❖ The density of all the silver complexes are comparatively high.
- ❖ The molecular conformation varies drastically in all three structures.
- ❖ Ag-N distances and X-Ag-Y ($^{\circ}$) angles in different silver complexes are comparable with other similar structures.
- ❖ The geometry around silver is, a distorted trigonal array and forms the infinite chain in the structure of AgSPZ (**Chap. 3**), whereas it adopts distorted tetragonal geometry in the structure of AGSCP (**Chap. 4**). In the molecular structure of AgSDZ (**Chap. 5**), the coordination of silver atom is pentadentate with the formation of chain in the lattice which reveals that stereochemistry of silver atom gets modified with change of ligand, solvents and the condition of crystallization.

B. Comparison of spectral data for Silver complexes

Comparison of few characteristic IR bands of all the three silver complexes along with respective ligand are summarized in **Table 10.4(a)**.

Table 10.4(a) Comparison of few characteristic IR bands of silver complexes

Assignment	Chapter 3		Chapter 4		Chapter 5	
	SPZ	AgSPZ	SCP	AgSCP	SDZ	AgSDZ
$\nu(\text{NH})$	3042	---	3138	---	3038	---
$\nu_{\text{as}}(\text{NH}_2)$	3476 3445	3441	3495	3380	3424	3391
$\nu_{\text{sy}}(\text{NH}_2)$	3353	3360	3394	3323	3355	3344
$(\text{SO}_2)_{\text{as}}$	1337	1346	1350	1302	1325	1293
	1314	1316	1330	1280	1262	1260
$(\text{SO}_2)_{\text{sy}}$	1148	1143	1191	1182	1156	1131
	1152	1124	1144	1167		

- ❖ The characteristic IR band for sulfonamide N-H is absent in all the three silver complexes revealing the deprotonation of -SO₂NH- moiety, thereby facilitating coordination of silver at the amido nitrogen. The NH₂ band is greatly affected due to complexation.

Comparison of significant NMR shift assignment of all the three silver complexes are tabulated in **Table 10.4(b)**.

Table 10.4(b) Comparison of significant shift assignment of silver complexes

Assignment	Chap.3		Chap.4		Chap.5	
	SPZ	AgSPZ	SCP	AgSCP	SDZ	AgSDZ
N(1)-H	9.88	---	11	---	11.25	---
C(2)-H/ C(6)-H	7.377	7.213	7.615	7.615	7.62	7.66
C(3)-H/ C(5)-H	6.607	6.572	6.599	6.572	6.56	6.43
Amino N-H ₂	6.097	---	6.101	5.872	6.00	5.7

- ❖ ¹H NMR spectra reveal that the peak for specific NH group is absent in all three silver complexes which support the coordination of silver at amido nitrogen.

In addition, close observations reveal the following interesting features:

- ❖ The entropy values for AgSPZ (**Chap.3**) and AgSCP (**Chap. 4**) are negative which suggest that these the complexes are stable.
- ❖ MIC result predicts that out of three, two silver complexes (**Chap. 3 & Chap. 5**) can be utilized as novel antibacterial agents.
- ❖ Conductivity measurement reflects the non-electrolytic nature of the ligands and their silver complexes.
- ❖ The two ring of the respective ligand in all three silver complexes are 67.57(13)° for **Chap.3**, 74.12(2)° for **Chap.4** and 74.6(2)° for **Chap.5**.

C. Comparison of data obtained by X-ray and by theoretical calculation for polymorphs

In the category-II, wherein four sulfonamide derivatives which are polymorphs, are investigated by X-ray diffraction technique. The comparative analysis of some general features like crystal system, density, space group, R index along with HOMO-LUMO energy and dipole moment have been tabulated in **Table 10.5**. **Table 10.6(a)** and **Table 10.6(b)** present the comparative list of significant bond lengths and bond angles of the different analogous polymorphs respectively. **Table 10.7(a)** and **Table 10.7(b)** summarize

comparative list of few significant torsional angle and dihedral angle of the different analogous polymorphs respectively.

Table 10.5 Comparison of few general features

	Chap.6	Chap.7	Chap.8	Chap. 9
	SMM	SMM-I	PHSCA	SP III
Crystal system	Monoclinic	Triclinic	Monoclinic	Monoclinic
Space group	P2 ₁ /n	P	P2 ₁ /n	C2/c
R [$F^2 > 2\sigma(F^2)$]	0.038	0.054	0.043	0.039
Goodness of fit (S)	1.05	1.06	1.05	1.08
Density (Mg/m ³)	1.510	1.451	1.414	1.458
HOMO energy	-8.5669	-5.7584	-6.9253	-5.2256
LUMO energy	-3.8183	-1.1664	-2.3565	0.1361
Dipole moment	6.0948	11.260	9.325	6.370

Table 10.6(a) Comparison of the significant bond lengths of the analogous polymorphs

Name of the compound	S1-O1	S1-O2	S1-N1	S1-C	N1-C	Ref.
Sulfachloropyridazine	1.433(6)	1.434(5)	1.647(2)	1.734(2)	1.394(3)	91
Sulfachloropyridazine Poly (I)	1.426(7)	1.434(5)	1.659(2)	1.737(2)	1.406(2)	92
Sulfapyridine Dioxane	1.448(2)	1.451(2)	1.600(2)	1.758(2)	1.356(3)	224
Sulfapyridine THF	1.440(2)	1.443(2)	1.614(2)	1.753(3)	1.352(3)	
Sulfameter Dioxane	1.432(2)	1.433(2)	1.639(2)	1.745(3)	1.393(3)	
Sulfameter THF	1.429(2)	1.434(2)	1.645(3)	1.741(2)	1.396(2)	
Sulfameter Poly (III) Mole A	1.423(4)	1.441(4)	1.638(17)	1.737(2)	1.401(2)	100
Sulfameter Poly (III) Mole B	1.432(5)	1.419(4)	1.651(2)	1.744(2)	1.396(2)	
Sulfadimethoxine Poly. (III)	1.419(8)	1.434(8)	1.646(2)	1.730(2)	1.356(2)	93
SMM	1.435(2)	1.435(3)	1.620(5)	1.756(6)	1.361(2)	
SMM Poly (I) Mole A	1.440(2)	1.443(2)	1.614(2)	1.753(3)	1.357(3)	
SMM Poly (I) Mole B	1.429(2)	1.429(2)	1.639(2)	1.739(3)	1.382(3)	Present Study
PHSCA	1.429(2)	1.426(2)	1.653(2)	1.753(2)	1.362(2)	
SP III	1.457(2)	1.441(2)	1.602(5)	1.751(2)	1.339(2)	

Table 10.6(b) Comparison of the significant bond angles of the analogous polymorphs

Name of the Compound	O1-S1-O2	O1-S1-N1	O1-S1-C	N1-S1-C	Ref
Sulfachloropyridazine	119.4(2)	108.2(2)	109.0(9)	106.7(9)	91
Sulfachloropyridazine Poly(I)	118.6(2)	108.1(2)	109.0(2)	106.4(9)	92
Sulfapyridine Dioxane	115.1(2)	104.7(2)	108.1(2)	107.8(2)	224
Sulfapyridine THF	117.0(1)	104.7(2)	108.2(2)	107.4(2)	
Sulfameter Dioxane	118.7(4)	108.6(4)	108.6(4)	107.6(3)	100
Sulfameter THF	118.5(8)	108.8(7)	108.8(7)	107.3(7)	
Sulfameter Poly (III) Mole A	118.4(8)	108.8(9)	108.8(9)	106.9(8)	
Sulfameter Poly (III) Mole B	119.7(9)	109.2(9)	109.2(9)	106.4(8)	
Sulfadimethoxine Poly.(III)	103.1(7)	106.1(6)	108.5(7)	114.0(1)	93
SMM	117.9(8)	104.0(8)	109.1(8)	105.8(8)	Present Study
SMM Poly (I) Mole A	116.5(2)	103.7(2)	109.4(2)	105.8(2)	
SMM Poly (I) Mole B	120.1(2)	103.6(2)	108.8(2)	107.3(2)	
PHSCA	119.7(9)	108.9(9)	108.7(8)	105.3(8)	
SP III	116.4(8)	111.5(7)	107.9(8)	106.1(8)	

Table 10.7(a) Comparison of the significant torsional angles of the analogous polymorphs

Name of the compound	Torsional angles (°)			Ref.
	O2-S1-N1-C	N1-S1-C1-C	C1-S1-N1-C	
Sulfachloropyridazine	53.7(2)	102.3(2)	-63.5 (2)	91
Sulfachloropyridazine Poly (I)	-62.2(2)	72.9(2)	54.7(8)	92
Sulfapyridine Dioxane	55.4(2)	-50.4(2)	-63.3 (2)	224
Sulfapyridine THF	49.6(2)	-76.3(2)	-67.8 (2)	
Sulfameter Dioxane	54.6(3)	104.0(2)	-63.6 (3)	100
Sulfameter THF	58.8(2)	107.8(2)	-59.7(2)	
Sulfameter Poly (III) Mole A	61.2(2)	-67.3(2)	-56.9(2)	
Sulfameter Poly (III) Mole B	-61.0(2)	-104.6(2)	56.7(2)	
Sulfadimethoxine Poly.(III)	-57.1(9)	-137.7(10)	-1.0(16)	93
SMM	44.6(2)	-72.5(2)	-44.32(6)	Present Study
SMM Poly (I) Mole A	-50.5(2)	67.4(2)	-134.8(2)	
SMM Poly (I) Mole B	42.6(3)	-73.9(2)	-91.4 (2)	
SP III	46.1(2)	-71.3(2)	102.1(4)	

Table .10.7(b) Comparison of the dihedral angle of the analogous polymorphs

Name of the compound	Between two rings	Ref.
Sulfachloropyridazine		91
Sulfachloropyridazine Poly (I)		92
Sulfapyridine Dioxane		224
Sulfapyridine THF		
Sulfameter Dioxane		
Sulfameter THF		100
Sulfameter Poly (III) Mole A		
Sulfameter Poly (III) Mole B		
Sulfadimethoxine Poly.(III)	77.5°	93
SMM	89.85 (8)°	
SMM Poly (I) Mole A	85.22(8)°	Present Study
SMM Poly (I) Mole B	78.88(13) °	
PHSCA	62.23(10)°	
SP III	86.35(8)°	

- ❖ From X-ray data, the dihedral angle between the phenyl and pyrimidine rings, ranging from 78.88(13) ° (molecule A) & 85.22(8)° (molecule B) in the structure of SMM-I to 89.85 (8)° in the SMM molecule.
- ❖ The lattice energies as obtained by PIXEL calculation reveal the strength of intermolecular interaction in terms of its energy and support the X-ray result. These observations are further strengthened by Hirshfeld surface analysis, the close contact interactions are represented by comparatively dark red region in d_{norm} surface.
- ❖ The docking study reveals that the presence of solvent water molecules into sulfamonomethoxine (SMM-I) change the molecular conformation and function relationship, compare to SMM molecule.

D. Percentage contribution of intermolecular interaction for the reported structures in the thesis through Hirshfeld surface analysis

Figure 10.3 is the comparison of percentage contribution of various close contacts for the reported structures in the thesis.

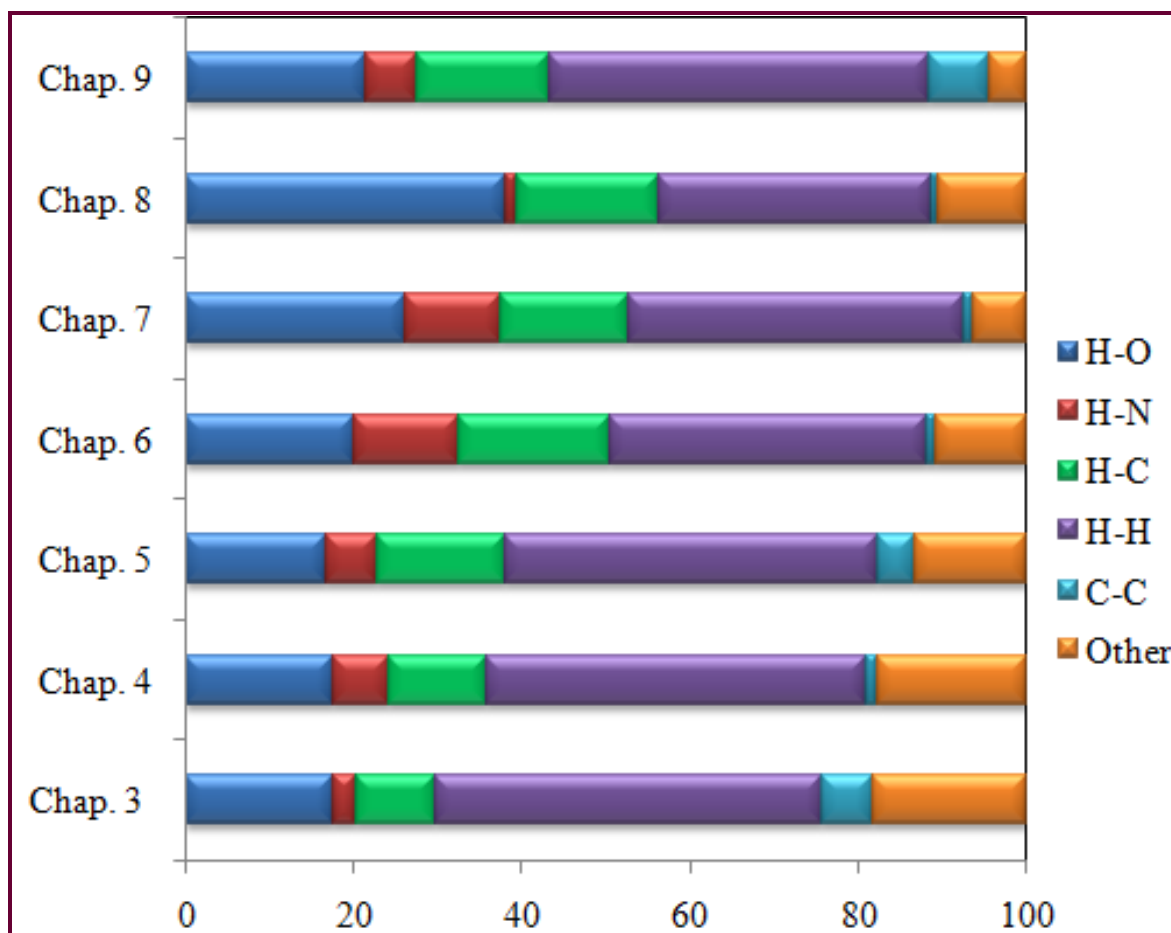


Figure 10.3 Percentage contributions of various close contacts for the reported structures in the thesis

- ❖ The observation for the contribution of short contacts reveals the fact that the contribution of H \cdots N contacts is very less in the case of all three silver complexes due to the coordination of nitrogen atom with silver, thereby decreasing the possibilities of nitrogen to form interaction.
- ❖ Presence of solvent water molecules in the structure of SMM-I (**Chap.7**) give rise more number of O-H \cdots O and N-H \cdots O interactions, compare to SMM (**Chap.6**) which has a lower contribution for H \cdots O contacts. It is noticeable that the presence of interactions due to water molecules led to reduction of the N \cdots H and H \cdots C percentage contribution to the total Hirshfeld surfaces in the SMM-I structure (**Chap.7**).

General Summary

- ❖ All the crystals are of good quality and diffract well. The $R_{\text{int}} < 0.05$ reveals that the qualities of data are good and the residual index for all these structures lie within 0.02-0.05 which is quite good.
- ❖ Small organic molecules prefer to stay in monoclinic system.
- ❖ All the six membered and five membered rings are planar in themselves in all the structures.
- ❖ Molecular conformation defined by torsional angles varies from molecule to molecule, revealing different molecular conformation with change in environment.
- ❖ Other interesting observation is that the C-H $\cdots\pi$ and $\pi\cdots\pi$ interactions play a very dominant role in stability of almost all the structures.
- ❖ Out of the seven crystal structure of sulfonamide derivatives, two molecules (**Chap. 3 and Chap. 7**) contain solvent water molecule. This water solvent plays an important role in stability of the molecule by forming number of intermolecular interactions.
- ❖ The S-N and S-C distances for silver complexes are shorter in comparison to respective ligands and polymorphs whereas, the S-O distance remains unaffected.
- ❖ The observation of dihedral angle reflects that the angles between two LSQ planes of silver complexes are comparatively shorter than those of polymorphs.
- ❖ Commonly, in all the silver complexes, the spectroscopic data are in good agreement with the crystal structure.
- ❖ The results from antimicrobial activity reveal the fact that the potency of the complexes varies in different sulfonamide against the different panel of bacteria.
- ❖ The root mean square error and correlation coefficients for all the structures predict the best matching between optimized geometry with those of experimental one, revealing the suitability of the applied basis set and confirms the suggested structure.
- ❖ Mulliken charge analysis for all the molecules strengthen the presence of the hydrogen bond interactions in crystalline phase.
- ❖ The analysis of Mulliken charge distribution reveals that in most of the structure the most negatively charged oxygen and nitrogen atoms belong to sulfonamide group and values for charge are comparable whereas, in the case of SMM-I, (Chap.7) the most negatively charged oxygen belongs from water molecule.

-
- ❖ HOMO and LUMO energy gap explains the eventual charge transfer interactions taking place within the molecule. For all the reported structure in the thesis, lower energy gap value is obtained.
 - ❖ The interaction energy of the molecular pairs via PIXEL calculation determines the strength of each interaction and the role of the weak interactions in the stability of crystal packing.
 - ❖ Hirshfeld surface and fingerprint plot analyses provide rapid quantitative insights into the intermolecular interactions in molecular solids. Close contacts like O...H, N...H and H...H in molecular solids have clear signatures in the fingerprint plots.
 - ❖ Using Glide suite of Schrödinger package, docking studies of the different polymorphs (reported in the thesis) have been carried out to understand the possibility of these molecules to act as an inhibitor.
 - ❖ Docking results suggest that molecular conformation may alter the structure-function relationship of same compound in different polymorphic state.